Modelling of hot pressing of paper

Modelling of hot pressing of paper

D. Bežanović[1], E.F. Kaasschieter[1] and M. Riepen[2]

[1] *Department of Mathematics and Computer Science, TU Eindhoven, P.O. Box 513, 5600 MB Eindhoven, The Netherlands*

[2] *TNO Institute of Applied Physics, Systems and Processes Division, P.O. Box 155, 2600 AD Delft, The Netherlands*

Abstract

In this paper a one-dimensional model for hot pressing of paper is considered. It is derived by supplying an energy equation to the previously derived three-phase model. Effects of thermal softening and plastic deformation of paper are taken into account. Numerical solutions are obtained using a 'saturation-upwind' method. The results show qualitative agreements with observed features of this process. They also suggest application of multinip or extended nip presses to improve pressing results.

1 Introduction

In the press-section of a paper machine, water is squeezed out of the wet paper by applying a sharp pressure pulse, as the paper together with the felt passes through the press-nip. The remaining water is removed in the dryer section. The low efficiency and the high costs of the dryer section is the reason why much efforts have been made to improve the rather simple and efficient press section. The limitations of experimental approaches (high processing speed, small paper thickness) motivate modelling of wet paper pressing.

One of the advanced technologies used in wet pressing is so-called hot pressing, where a combined action of pressing and a high temperature is

used to improve the pressing results. In addition to a sharp pressure pulse, web paper is exposed to a heat flux from a preheated press roll. A high temperature improves dewatering by (see for instance [6]):

- reducing the flow resistances of water and air by reducing their viscosities,

- thermal softening of the fiber network, allowing for improved web consolidation.

In case of impulse drying, where temperatures exceed 100°C and go up to 300°C, additional effects occur:

- increased the hydraulic pressure gradient via steam formation,

- increased evaporation after the press nip.

Riepen [13] models mathematically hot pressing of paper, by proposing an essentially two-phase (water and solid) model. The model is applicable for completely saturated paper, while the effects of air in felt are taken into account by assuming that water and air are distributed in an a priori known way. The phase transition of water is also taken into account, i.e. the model describes also impulse drying. Using homogenization, Bloch [6] derives a model of heat transfer through nonsaturated porous media and applies it to hot pressing of paper. An overview of the impulse drying research was made by Van Lieshout [10].

In this paper we propose a three-phase model for hot pressing of paper, i.e. we restrict ourselves to temperatures below 100°C. Basically we supply an already derived model from [5] with energy equations for the porous media (paper and felt) and the press roll. The temperature dependence of the flow equations comes through the fluid viscosities, air density and thermal softening of paper. At the other side the convection of temperature depends on the flow of fluids, while the effective thermal coefficients of paper and felt depend on the composition of the water-air-solid mixture.

In Section 2 we introduce the model (consisting of flow and temperature equations and a set of initial, boundary and cross conditions) and outline its physical and the mathematical nature. In Section 3 we present and comment on computational results of typical examples of hot pressing. Conclusions are given in Section 4.

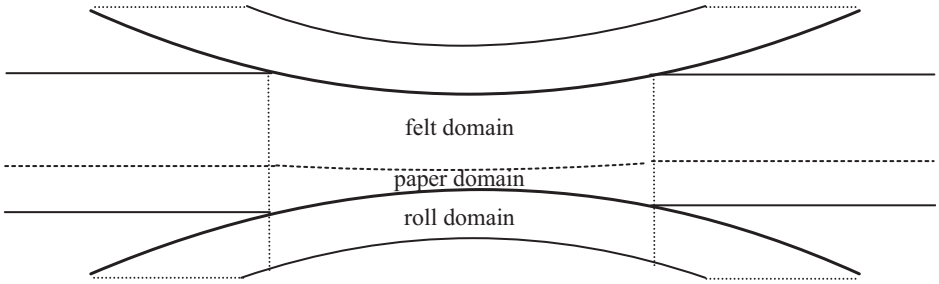

Figure 1: Scheme of the press section of paper machine.

2 The model

The flow equations model flow of the fluids and compression of the layers. Since we will consider the case of impermeable press rolls, the flow problem is restricted only to the paper and the felt domain (see Figure 1). On the other hand, as we will see, the temperature problem considers the temperature distribution throughout three domains: lower roll, paper and felt.

2.1 Flow equations

In this section we briefly introduce the three-phase flow model that was derived and studied in more details in [4, 5], and adjust it to non-isothermal conditions.

Paper and felt are considered to be deformable porous layers. The permeability changes with the deformation, giving a relation between permeability and porosity. Water and solid are assumed to be intrinsically incompressible, while air is assumed to be an ideal gas. Having in mind the typical geometry of the press-nip (see [9, 15] for instance) we consider only the flow and deformation in the vertical (transversal) direction, obtaining a one-dimensional, transversal model.

The governing equations are mass balance equations for water, air and solid, Darcy's equations for water and air and the balance of total momentum. The closure is given by a set of state equations (ideal gas assumption for air, intrinsic permeability as a function of porosity, relative permeabilities as functions of water saturation, structural pressure as a function of strain).

It turns out that, instead of the porosity ϕ, the scaled void ratio u defined

by

$$u = (1 - \phi_0)\frac{\phi}{1 - \phi}$$

is more convenient to use. Darcy's laws for water and air read

$$q_j = -\frac{k(u)k_j^r(s)}{\mu_j}\frac{\partial p_j}{\partial z},\ j = w, a.$$

Here q_j, $j = w, a$ (subscripts w and a refer to water and air, respectively) are specific discharges relative to the solid structure, z is the vertical (transversal) coordinate, s is the water saturation, μ_j are viscosities, k is the intrinsic permeability and k_j^r are relative permeabilities. The specific choice of the functions $k(u)$ and $k_j^r(s)$ will be given in Section 3.

The mechanical response of the solid skeleton of felt is assumed to be perfectly elastic and independent on temperature. The second assumption does not pose a big restriction since temperature changes in felt are limited (see Section 3). These assumptions yield, as in [4, 5], a structural pressure-strain relation. Using the relation between strain and void ratio (see [3])

$$\epsilon = u - u_0,$$

we obtain a structural pressure-void ratio relation for felt:

$$p_s^f = p_{s0}^f \left(u^{-q^f} - u_0^{-q^f}\right),\ q^f > 0. \tag{1}$$

The superscripts p and f refer to paper and felt, respectively.

Wet paper shows a more complicated mechanical behaviour. First, for higher temperatures wet paper softens, i.e. the Young modulus of the fibrous network decreases, see [2, 6]. Back [2] explains this thermal softening by the reduced inter-fibre and intra-fibre hydrogen bonding. Having in mind that the Young modulus is given as $dp_s/d\epsilon$ (or equivalently dp_s/du), we model this phenomenon by introducing an additional temperature dependence in the structural pressure-void ratio relation:

$$p_s^{com,p}(u) = A(T)p_{s0}^p \left(u^{-q^{com,p}} - u_0^{-q^{com,p}}\right),\ q^{com,p} > 0, \tag{2}$$

where the decreasing function $A(T)$ will be specified in Section 3. The appearance of superscript *com* suggests that this relation is valid during the compression (loading) phase.

After the press-nip wet paper does not return to its initial thickness (see [9] for instance), i.e. both semi-permanent and permanent deformations occur. Semi-permanent deformations are associated with a delayed response during unloading (releasing of pressure). El-Hosseiny [7] reports that this phenomenon occurs due to the flow of fluids through the pores, while the plain fibrous structure does not exhibit visco-elastic behaviour. Apart from this, wet paper is partially permanently deformed, i.e. it never regains its original thickness after release of pressure. Therefore relation (2) is used only in the compression phase. In the expansion phase, as in [5] and following the idea from [9], a different stress-void ratio relation is used.

We introduce a parameter ϵ_{pl} and consider a particle that, at the state of maximal deformation has the strain equal to ϵ_1. We assume that after releasing of the pressure this particle returns to state with strain equal to $\epsilon_2 = \epsilon_{pl}\epsilon_1$, see Figure 2. Letting $u_1 = \epsilon_1 + u_0$ and $u_2 = \epsilon_2 + u_0$, during expansion (unloading) we use the relation

$$p_s^{exp,p}(u) = A(T)p_{s0}^p \left(u^{-q^{exp,p}} - u_2^{-q^{exp,p}}\right),\ q^{exp,p} > 0, \tag{3}$$

where $q^{exp,p}$ is taken such that $p_s^{com,p}(u_1) = p_s^{exp,p}(u_1)$. Although every particle has a different compression history and begins to expand at a different moment, in order to simplify modelling we use relation (3) for all particles, from the moment when the complete paper layer starts to expand. The expression for paper thickness will be given later, in material coordinates.

Water and air viscosities are temperature dependent ($\mu_j = \mu_j(T)$, $j = w, a$). The functional dependences will be specified in Section 3.

Assuming, as in [9], local pressure equilibrium of fluids we write

$$p_a = p_w =: p_f, \tag{4}$$

where p_f denotes the average pressure of the water-air mixture. With this assumption, the total applied pressure p_T is distributed over the solid and fluid phases accordingly to Terzaghi's principle [1], implying

$$p_T = p_s + p_f. \tag{5}$$

Air is considered to be a perfect gas, implying a linear relation between density and pressure. In addition, the temperature dependence is taken into account. The specific choice of the function

$$\rho_a = \rho_a(p_a, T) \tag{6}$$

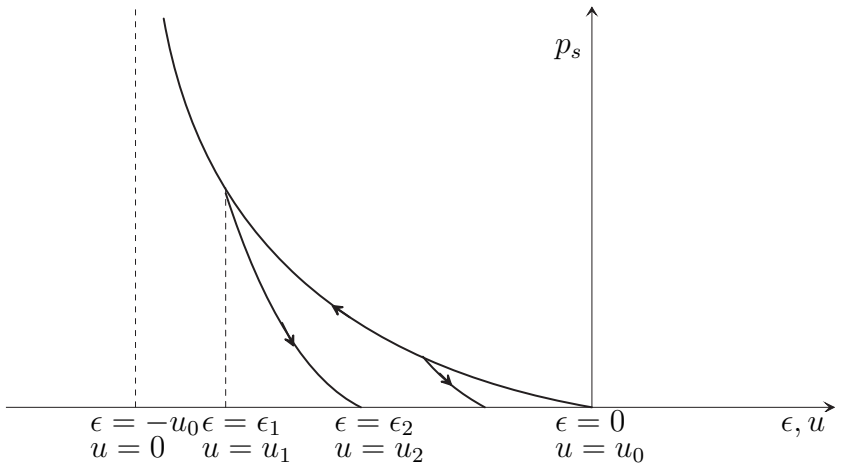

Figure 2: Pressure-strain (void ratio) curves for the compression and expansion phase, for a fixed temperature.

is given in Section 3.

Using Terzaghi's principle (5), a given total pressure as a function of time ($p_T = p_T(t)$) and using (1) (for felt) and (2) during the paper compression and (3) during the paper expansion, we express the fluid pressure as

$$p_f = p_f^i(u,t) = p_T(t) - p_s^i(u),\ i = p, f.$$

This relation, together with (6) and (4) yields relation

$$\rho_a = \rho_a^i(u,T,t),\ i = p, f.$$

To fix the (paper and felt) domain we use the (scaled) vertical material coordinate x corresponding to the initially undeformed configuration. As in [4] we have

$$\frac{\partial}{\partial z} = \frac{\partial}{\partial x}\frac{\partial x}{\partial z} = \frac{1}{h_0(1+\epsilon)}\frac{\partial}{\partial x} = \frac{1}{h_0(1-u_0+u)}\frac{\partial}{\partial x}.$$

Here $h_0 = h_0^p + h_0^f$, where h_0^p and h_0^f are the initial thicknesses of paper and felt, respectively. Redefining the time by taking $t := t/t_{fin}$, where t_{fin} is the total time of press nip, the paper and felt domains from Figure 1 transform to the rectangles Q^p and Q^f, from Figure 3.

As in [5] we rewrite the governing and the state equations into a system of two partial differential equations:

$$(us)_t = \left(C_w^i(u,s,T)u_x\right)_x,\ i = p, f \text{ (water equation)}, \tag{7}$$

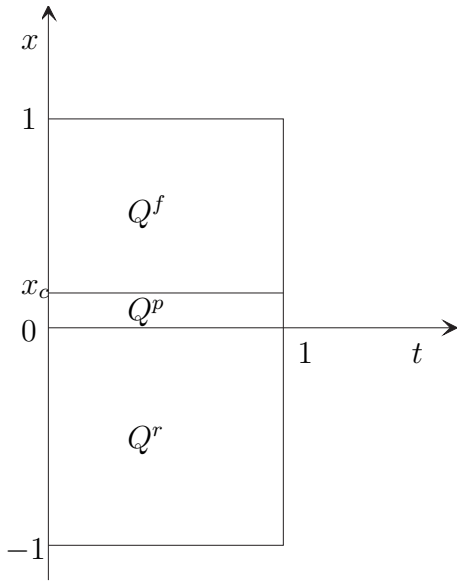

Figure 3: Computational domains Q^r, Q^p and Q^f. $x_c = h_0^p/h_0$ corresponds to the paper-felt contact.

$$(u(1-s)\rho_a(u,T,t))_t = (\rho_a(u,T,t)C_a^i(u,s,T)u_x)_x,\ i=p,f \text{ (air equation)}, \tag{8}$$

where

$$C_j^f(u,s,T) = \frac{t_{fin}}{h_0^2}\frac{k^f(u)k_j^{rf}(s)}{\mu_j(T)}q^f p_{s0}^f u^{-q^f-1},\ j=w,a,$$

and

$$C_j^p(u,s,T) = \frac{t_{fin}}{h_0^2}\frac{k^p(u)k_j^{rp}(s)}{\mu_j(T)}A(T)q^{\alpha,p}p_{s0p}u^{-q^{\alpha,p}-1},\ j=w,a.$$

Equations with superscript of the coefficients $i=p$ and $i=f$ are considered in the paper (Q^p) and the felt (Q^f) domain, respectively. In $q^{\alpha,p}$ we take $\alpha = com$ at the compression and $\alpha = exp$ in the expansion phase. It is straightforward to show that the thickness of paper is given by

$$h_p(t) = h_{0p}(1-u_{0p}) + h_0\int_{x_{c1}}^{x_{c2}} u(\eta,t)\ d\eta.$$

Clearly $h_p'(t) < 0$ is a criterion for the compression phase of the paper layer and $h_p'(t) > 0$ for its expansion phase.

Remark 2.1 *In the derivation of equations (7) and (8) we have neglected the flow of fluids caused by temperature gradients. In other words, we have used the approximation*

$$\frac{\partial}{\partial x} A(T) p_s^i(u) \approx A(T) p_s^{i\prime}(u) u_x, \;\; i = p, f.$$

This is justified by the numerical results implying that $A(T)p_s^{i\prime}(u)u_x$ is mainly one order of magnitude larger than $A'(T)p_s^i(u)T_x$.

Remark 2.2 *(Nature of the flow model (7)–(8))*

Let us assume for the time being that the temperature distribution is known. We are left with a closed system of two partial differential equations (7) and (8) in terms of void ratio and saturation. The mathematical nature of this system and the properties of the solutions are not immediately clear. Here we omit the superscripts $i = p, f$ since this consideration applies both to the paper and to the felt.

Following the procedure from [4, 5], by introducing a new unknown r through a suitable chosen transformation $r = r(u, s)$, the system (7) and (8) can be transformed into a parabolic-hyperbolic system in terms of u and r:

$$\begin{cases} u_t = a(r, u, u_x, t) u_{xx} + b(r, u, u_x, t), \\ r_t + c(r, u) u_x r_x = d(r, u, u_x, t), \end{cases}$$

for some nonlinear coefficients a, b, c and d. From the $r-$equation it follows that the characteristic speed for r is

$$\dot{x}(t) = c u_x. \tag{9}$$

Smoothness of the transformation $r = r(u, s)$ implies that (9) is also the characteristic speed of s. No-flow conditions at $x = 0$ and $x = 1$ can be expressed as $u_x = 0$, implying that no boundary conditions for r (and s) are needed, since the corresponding characteristics at $x = 0$ and $x = 1$ are parallel to the $t-$axis and thus do not enter into the computational domain. Furthermore, the hyperbolic nature of the equation for r explains also why only a single cross condition is required for this variable (and thus for s) at the paper-felt interface. It also explains why we may expect shocks for r and in s. The choice of the numerical scheme will (by means op suitable upwinding) account the hyperbolic behaviour of the equations in s.

2.2 Temperature equations

In the situation of our interest, the lower roll (see Figure 1) is preheated, while paper, felt and the upper roll are assumed to be initially cold (i.e. at the ambient temperature). The thickness of the felt layer suggests that its upper part and the upper roll do not change their temperatures in the press-nip (this is verified by numerical experiments). Therefore the temperature problem can be restricted to the lower roll and the paper and felt domain. We introduce here temperature (energy) equations for porous layers (paper and felt) and for the steel press roll.

Temperature equation for the paper and the felt

We consider the porous media (paper or felt) as mixtures of three intrinsic phases: solid, water and air. We take into account only heat transfer through all intrinsic phases by conduction and through fluid phases by convection.

We neglect dispersion of heat in fluids and heat radiation between solid particles. Furthermore we neglect, as in [6, 13], the temperature differences beween the intrinsic phases. This assumption depends on the type of porous medium, the ranges of temperatures and the space and time scales involved. Naturally, it is more acceptable in the case of 'fine' porous media and for 'slow' processes, where the total time is much larger than the time needed for solid and fluid temperatures to approach each other.

The conduction arises from the exchange of kinetic energy by the colliding molecules. It is macroscopically described by Fourier's law stating that the conduction flux is a linear function of the temperature gradient. As the fluid (water and air in our case) moves, it carries its own heat content with it. This results into a macroscopical convective term in the energy (temperature) equation.

As in [13], only transversal transport of energy is taken into account, which is justified by the following facts. The numerical experiments show that the convection is in general the dominant mode of the heat transport. At the other hand the transversal flow (and consequently the heat convection) is one order of magnitude larger than the the longitudinal flow and heat convection.

Under these assumptions, an averaging procedure as in [1] leads to the

temperature equation for paper and felt:

$$C^{eff,i}T_t + \sum_{j=w,a} \rho_j C_j q_j T_z = \left(\lambda^{eff,i} T_z\right)_z, \ i = p, f, \tag{10}$$

where ρ_w is the water density and C_j, $j = w, a$ are the phase heat capacities. The coefficients $C^{eff,i}$ and $\lambda^{eff,i}$ respectively are the effective heat capacity and effective heat conductivity, taken as the volume average of the corresponding phase quantities:

$$C^{eff,i} = \sum_{j=w,a} \phi_j \rho_j C_j + \phi_s \rho_s^i C_j^i, \ i = p, f,$$

and

$$\lambda^{eff,i} = \sum_{j=w,a} \phi_j \lambda_j + \phi_s \lambda_s^i, \ i = p, f, \tag{11}$$

where ϕ_j is the volume fraction of phase j and ρ_s is the intrinsic density of solid particles. Relation (11) implies that a parallel conduction model is adopted, i.e. the conduction through all intrinsic phases is assumed to occur separately and simultaneously. There are alternative conduction models (serial for instance) implying alternative formulas for λ^{eff} as averages of λ_j, $j = w, a, s$.

Using the scaled material coordinate x and the rescaled time t as in Section 2.1, equation (10) becomes

$$C^{eff,i}T_t + \sum_{j=w,a} \frac{t_{fin}}{h_0} \frac{\rho_j C_j q_j}{1 - u_0 + u} T_x = \frac{1}{1 - u_0 + u} \left(\frac{t_{fin}}{h_0^2} \frac{\lambda^{eff,i}}{1 - u_0 + u} T_x \right)_x, \ i = p, f. \tag{12}$$

Temperature equation for the press roll

Since the press roll does not experience deformation, vertical spatial coordinate x is used. This coordinate is scaled by dividing the nonscaled vertical coordinate z by the total thickness of the roll h^r. Scaling time as in Section 2.1 the temperature equation for steel roll reads

$$\rho^r C^r(T) T_t = \left(\frac{t_{fin}}{(h^r)^2} \lambda^r T_x \right)_x, \tag{13}$$

where ρ^r, c^r and λ^r are the density, heat capacity and heat conductivity of steel, and the subscript r refers to (lower) roll. This equation is considered in the rectangular roll domain Q^r from the Figure 3.

2.3 Initial, boundary and cross conditions

In order to solve the flow and the temperature problem, apart from the equations (7), (8) and (12) and (13) we need to specify a set of initial, boundary and cross conditions.

Initial condition ($t = 0$)

It is assumed that the initial distribution of void ratio in paper and felt is known and uniform. In particular, the values of void ratio in both layers correspond to the undeformed state. In addition, the initial temperature of the lower roll, paper and felt is assumed to be known (the paper and the felt are assumed to have the ambient temperature).

Lower boundary of the roll ($x = -1$)

The temperature of the lower boundary of the press roll is assumed to be constant and equal to the initial temperature of the roll. This approximation is justified by the thickness of this roll and the short nip residence time and it is verified by numerical experiments.

Roll-paper contact ($x = 0$)

Impermeability of the press roll implies no-flow boundary condition at paper-roll interface, which can be expressed as (see [4, 5])

$$u_x = 0. \tag{14}$$

Therefore the flow problem is restricted to the paper-felt domain. Due to the hyperbolic nature of the flow equations in s (Remark 2.2), no boundary conditions are needed for s. Using the no-flow condition (14), the conservation of energy implies (taking into account different scalings of the roll and

the paper-felt domains)

$$\frac{1}{h^r} k^r T_x \Big|_{x=0^-} = \frac{\lambda^{eff,p}}{h_0(1-u_0^p+u)} T_x \Big|_{x=0^+} \quad \text{for all} \quad t.$$

Furthermore the temperature is assumed to be continuous at the paper-roll contact:

$$T(0^-,t) = T(0^+,t) \quad \text{for all} \quad t.$$

Paper-felt contact ($x = x_c$)

At the paper-felt interface continuity of the structural pressure p_s and the water and air mass discharges $\rho_j q_j$, $j = w, a$, is assumed (see [4, 5] for more details). The temperature is assumed to be continuous, i.e.

$$T(x_c^-,t) = T(x_c^+,t), \quad \text{for all } t.$$

The conservation of energy implies

$$\left\{ \sum_{j=w,a} \frac{t_{fin}}{h_0} \rho_j C_j q_j T + \frac{t_{fin}}{h_0^2} \frac{\lambda^{eff,p}}{1-u_0^p+u} T_x \right\} \Big|_{x=x_c^-}$$
$$= \left\{ \sum_{j=w,a} \frac{t_{fin}}{h_0} \rho_j C_j q_j T + \frac{t_{fin}}{h_0^2} \frac{\lambda^{eff,f}}{1-u_0^f+u} T_x \right\} \Big|_{x=x_c^+}.$$

Continuity of T, q_j and ρ_j, $j = w, a$, reduces the above condition to

$$\frac{\lambda^{eff,p}}{1-u_0^p+u} T_x \Big|_{x=x_c^-} = \frac{\lambda^{eff,f}}{1-u_0^f+u} T_x \Big|_{x=x_c^+}.$$

Upper boundary of the felt ($x = 1$)

Impermeability of the press roll implies a no-flow condition (14) at $x = 1$. Additionally we assume that the upper boundary of the felt stays at the same (ambient) temperature during the complete press nip. This assumption is also justified by the numerical experiments.

3 Computational results

We first briefly explain the numerical method. Then we give the solution of a typical example, comment the main features of the model and compare the results with other experimental and modelling studies.

3.1 Numerical method

In order to compute the numerical solutions of system (7), (8) and (12), a generalization of the numerical method from [5] is used.

For the equations (7) and (8) the same explicit scheme, derived using finite volumes, is used. The scheme takes into account the parabolic dependence of the flow equations in u and the hyperbolic dependence in s (see Remark 2.2): at the interfaces between control volumes u is approximated by centered approximations while its $x-$derivatives are approximated by central differences; s and s_x are approximated in an upwind manner, depending on the direction of the flow, i.e. the sign of u_x.

The explicit Euler method for time integration of (12) is used. The convection term is approximated in an upwind way (depending on the direction of the flow), while the conduction term is approximated using central differences. Namely, the convection of heat physically depends only on upwind values, while the conduction depends on values from both sides of a given point inside a medium.

Temperature equation (13) for the press roll is discretized straightforwardly, using an explicit scheme combined with finite volumes, and central difference approximation of the x-derivatives of T.

The initial and boundary conditions from Section 2.3 are discretized straightforwardly (details for the pressure and flow conditions are given in [4]).

3.2 Numerical solution

We consider a typical example of hot paper pressing, where the lower press roll which is in contact with paper (see Figure 1) is preheated.

First we specify the state equations from Section 2. For the intrinsic and the relative permeabilities we take (see for instance [1, 8]):

$$k = k(u) = k_0 \frac{u^3}{(1-\phi_0)^2(1-\phi_0+u)} \quad \text{(Kozeny-Carman)},$$

and

$$k_w^r(s) = s^{\frac{2+3\nu}{\nu}},\ k_a^r(s) = (1-s)^2(1-s^{\frac{2+\nu}{\nu}}),\ \text{(Brooks-Corey)}.$$

The ideal gas equation (6) is taken as

$$\rho_a = \left(\frac{p_T(t) - p_s(u) - p_{a0}}{\gamma_1} + \rho_{a0}\right)(-\gamma_2(T - T0) + \gamma_3),\ \gamma_1, \gamma_2 > 0.$$

parameter		paper	felt	(lower) roll
u	$[\cdot]$	0.55	0.45	–
s	$[\cdot]$	0.85	0.45	–
T	[°C]	20	20	100

Table 1: Initial conditions.

The fluid viscosities-temperature relation is taken in the form

$$\mu_j(T) = \mu_{j0} e^{-c_j(T-T_0)},\ c_j > 0,\ j = w, a.$$

The coefficient c_j is taken to be equal for water and air. The function $A(T)$ from (2) and (3) is taken as

$$A(T) = e^{-c_A(T-T_0)},\ c_A > 0.$$

Here T_0 is the ambient temperature, taken to be equal to 20°C. Clearly $A(T_0) = 1$, while c_A is chosen such that $A(100) = c_{com}$. The coefficient $c_{com} \in (0, 1]$ thus controls the magnitude of thermal reduction of the Young modulus and, in particular, $c_{comp} = 1$ implies the absence of thermal softening.

The total pressure is taken as a function of time:

$$p_T(t) = p_{T0} \sin^2(t),\ t \in [0, 1].$$

The temperature dependence of the thermal coefficients is neglected.

The values of the initial conditions are given in Table 1, while the numerical values of all parameters are given in Table 2.

The primary output of the model are distributions of temperature, water saturation, void ratio and air density in material coordinates. Using the transformation to spatial coordinates other important quantities (the thickness, total mass of water and deformations of paper) are computed.

The computational results are displayed in Figures 4, 5 and 6. For a better understanding of the results we can consider the time t as a scaled horizontal (longitudinal) coordinate. As in the case of cold pressing [5] the main features of wet pressing are reflected. In the beginning of the nip the flow of water from paper to felt is negligibly small (see the solid line in Figure 6(b)). The flow is maximal around the mid-nip (middle of the nip), when the water saturation (Figure 5) and the fluid pressure in paper reach the highest values. In our case no rewetting of paper occurs in the second half of the nip,

parameter	value		
p_{a0} [MPa]	0.1		
ρ_{a0} [kg m^{-3}]	1.2		
γ_1 [$\cdot$]	26		
γ_2 [$\cdot$]	0.003		
γ_3 [$\cdot$]	1.06		
t_{fin} [s]	$2.4 \cdot 10^{-2}$		
μ_{w0} [kg m^{-1}s^{-1}]	10^{-3}		
μ_{a0} [kg m^{-1}s^{-1}]	$1.8 \cdot 10^{-5}$		
$c_w (= c_a)$ [$\cdot$]	0.016		
c_{com} [$\cdot$]	0.8		
c_A [$\cdot$]	0.003		
p_{T0} [MPa]	5		
	Paper	*Felt*	
h_0 [mm]	0.17	1.5	
p_{s0} [MPa]	0.23	0.5	
q [$\cdot$]	4	3.5	
k_0 [m^2]	$5 \cdot 10^{-15}$	$1.7 \cdot 10^{-14}$	
ν [$\cdot$]	3	2	
ρ_s [kg m^{-3}]	1500	100	
λ_s [J m^{-1} s^{-1} kg^{-1}]	0.33	0.03	
C_s [J kg^{-1} K^{-1}]	$1.33 \cdot 10^3$	$2 \cdot 10^3$	
	water	*air*	*roll*
λ [J m^{-1} s^{-1} K^{-1}]	0.602	0.026	50
C [J kg^{-1} K^{-1}]	$4.18 \cdot 10^3$	10^3	$0.5 \cdot 10^3$
ρ [kg m^{-3}]	10^3	–	$7.8 \cdot 10^3$

Table 2: Parameter set used in computations.

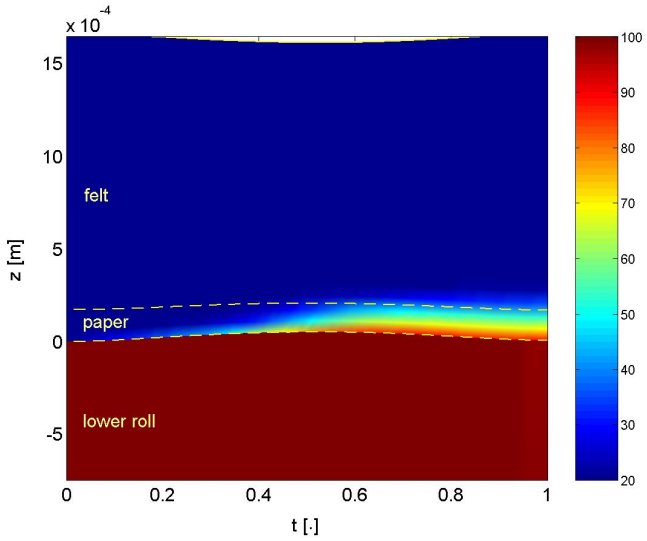

Figure 4: Temperature distribution in the upper part of the lower roll, paper and felt domain, in the spatial coordinate z.

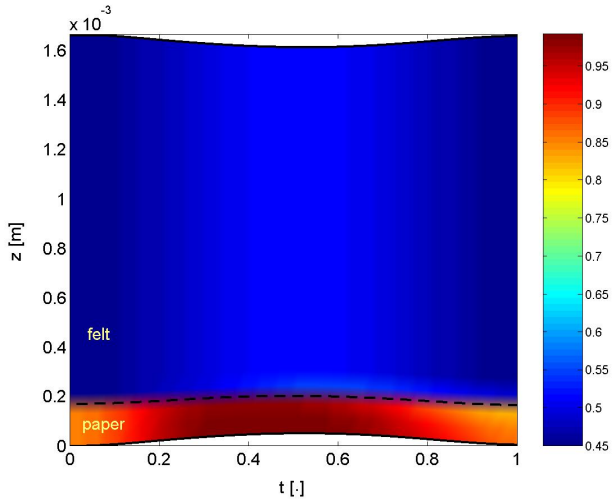

Figure 5: Water saturation in paper and felt domain in the spatial coordinate z.

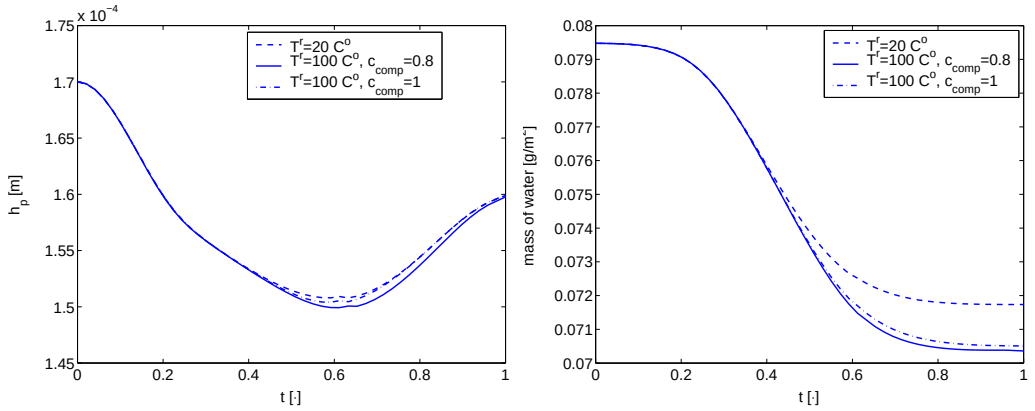

(a) Thickness of paper.

(b) Mass of water in the paper.

Figure 6: Comparisons of the cold and hot pressing (with and without effects of thermal softening).

when the layers expand (solid-line plot line in Figure 6(b) is decreasing for all t). In fact, as it was verified in [5], if the plastic paper deformations are neglected a small paper rewetting occurs just before the end of the press-nip.

We now comment the mechanisms of the heat transport from the pre-heated lower roll into the paper-felt domain (Figure 4). The heat is initially transported to the paper only by conduction. As soon as the high temperature arrives deeper inside the paper and when the fluid flow becomes more intense (just before the mid-nip), the fluids bring along the high temperature in the direction of the felt, and the convection becomes the dominant mode of heat transfer. The fluid flow, and consequently the convective energy transport, is maximal around the mid-nip.

In Figures 6(a) and 6(b) the evolutions of the paper thickness and the water content for the case of the cold pressing ($T^r = 20°\text{C}$) and the hot pressing ($T^r = 100°\text{C}$) are displayed. To understand the effects of thermal softening of the paper, we add the plots for the case of the hot pressing but when thermal softening is not taken into account ($c_{com} = 1 \Leftrightarrow A \equiv 1$).

Due to improved fluid flow caused by the reduced viscosities paper attains the smallest thickness close to the mid-nip for the case of the hot pressing. The mid-nip thickness of paper is smaller if the thermal softening of paper is taken into account. The difference in the final paper thickness in all three cases is small. The final paper thickness is, knowing the magnitude of the

maximal compression, possible to estimate (approximately), and it follows from the pressure conditions at paper-felt interface.

The effects of high temperatures on the dewatering of paper (Figure 6(b)) are significant. Differences between the flow in the cold and the hot pressing occur clearly only when the heat is well distributed in the paper-felt domain (in the second half of the press-nip). The temperature dependence enters into the flow equations (7) and (8) through the ratio $A(T)/\mu_j(T)$, which is an increasing function. Therefore, when the temperature increases, the diffusion coefficients of the flow equations increase, and the flow is improved. Since no rewetting occurs, i.e. during the whole press-nip fluids flow from paper to felt, an improvement in flow directly implies an improvement in the paper dryness.

Thermal softening has a twofold influence on dewatering of paper. The first effect is positive: when temperature increases, the paper softens and attains a smaller thickness (comparing to the case $c_{com} = 1$). The second effect is negative: when temperature increases, the diffusion coefficients in the flow equations become smaller (than in the case $c_{com} = 1$) which reduces the flow. In Figure 6(b) we see that in this case positive effects dominate, i.e. the final water content is smaller if thermal softening is taken into account.

The effects of high temperatures are however restricted only to the second half of the nip, when the temperature is well distributed inside the paper. One way to take more advantage of high-temperature effects would be to use an extended press nip, i.e. to continue pressing when the high temperature is well distributed inside the paper. On the other hand, since paper machines have in general several press-nips, in all following press-nips paper enters already preheated and the high-temperature effects are present in the whole nip. In the next subsection, we will actually apply our model to describe multinip hot pressing.

Our solutions are in qualitative agreement with the results of Riepen [13], who also observed that in the initial stage of the nip conduction is the mean mode of the heat transport, while in the later stage heat is mainly convected by the fluid.

3.3 Modelling of multinip hot pressing

As it was already mentioned, a press section often consists of several press nips. However, the efficiency of every successive press-nip is smaller than the efficiency of the previous one. The main reasons for this are the consolidation

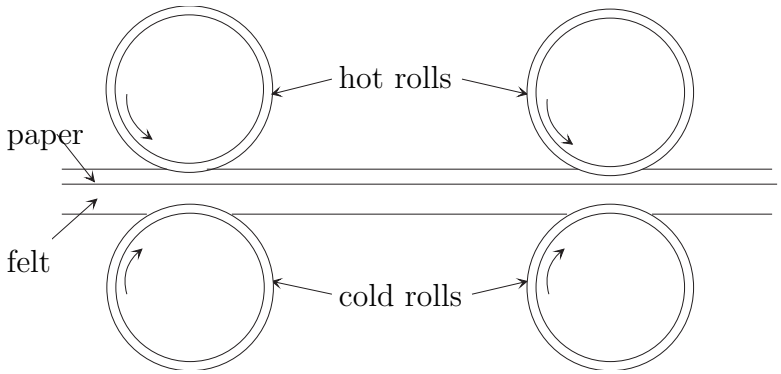

Figure 7: Scheme of two successive hot press nips.

of paper due to plastic deformations and the reduced amount of water in paper. To get an idea about the effects arising in multinip pressing, we employ our model to compute the dewatering for the case of two subsequent press nips.

We assume that not-preheated paper enters into the first nip, see the scheme in Figure 7. After leaving the first nip paper is carried by the felt towards the second nip, which is assumed to be at 1 m distance from the first nip. In both press-nips only the upper roll, which is in contact with paper, is preheated (to 100°C).

The pressing in the first nip is already modelled in the previous subsection. We neglect any flow inside paper and felt on the way between two nips, motivated by the following arguments. First, the total time is small and thus capillary effects, that are characteristic for much slower processes, can be neglected. Second, the void ratio reaches at the end of the first nip values that correspond to zero structural pressure. Therefore, between two nips (when the external pressure is released) there is no flow caused by relaxation of these layers. We compute however the temperature redistribution in the paper-felt domain and the effects of cooling of paper by surrounding air. Although being partially cooled, paper enters the second nip preheated. Moreover, due to the redistribution in the region between the nips, high temperature penetrates into the region around paper felt interface, where the flow is the most intensive. This has positive effects on the pressing in the second nip.

Our computations show that the application of high temperatures improves the efficiency of the later (second, third etc.) nip, since paper enters these nips already preheated. In our example, hot pressing in two successive

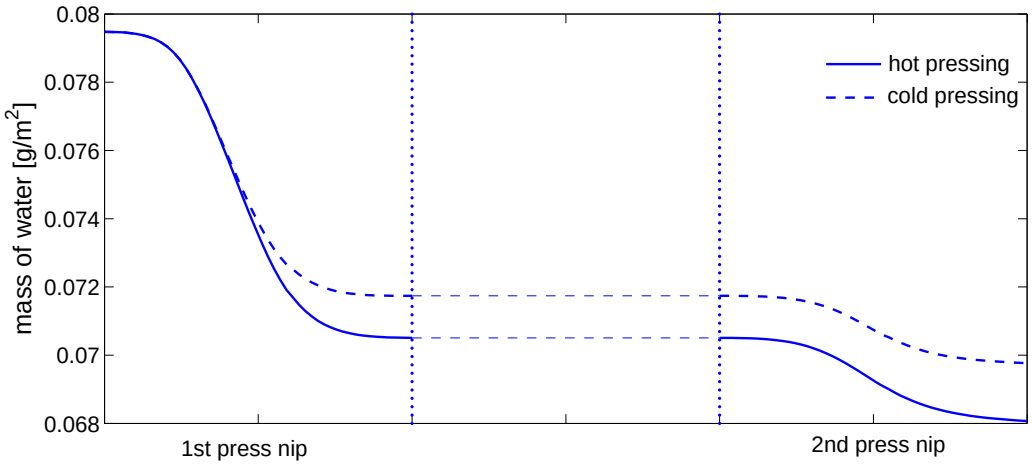

Figure 8: Evolution of water content in paper in case of two successive nips, for hot and cold pressing.

nips reduces the amount of water for 14.4% (first nip reduces water amount for 11.3%). In the case of cold pressing, water content is reduced for 12.2% in total (9.7% after the first nip). Therefore, applying hot pressing more water is removed in the press section of the press machine.

4 Conclusions

In this study we have proposed a model for hot pressing of paper, basically by extending our previous model for wet paper pressing with energy equations. Comparisons of the computational results with modelling and experimental studies show that the model captures fundamental features of the process of hot pressing. Apart from known effects of enhancing flow by reducing fluid viscosities, the mechanisms of the influence of thermal paper softening on pressing results are illuminated. The proposed numerical model is a good tool to study the influence of parameters and pressing regimes (for instance: different total press curves associated with extended and multi-nip presses etc.). In particular, the computations suggest that application of the extended press-nips and pressing by several successive nips improve efficiency of hot pressing.

One of the following steps to improve the proposed model can be to include the effects of water phase transition and make it applicable for tem-

peratures higher than 100°C, i.e. for impulse drying.

References

[1] J. Bear, *Dynamics of Fluids in Porous Media*, Elsevier, New York (1972).

[2] E.L. Back, Steam boxes in press sections-possibilities and limitations, *Appita* **41**(3), 217-223, 1998.

[3] D. Bežanović, C.J. van Duijn and E.F. Kaasschieter, Analysis of paper pressing: the saturated one-dimensional case, to appear in *Journal of Applied Mathematics and Mechanics*.

[4] D. Bežanović, E.F. Kaaschieter and C.J. van Duijn, Analysis of wet pressing of paper: the three-phase model. Part I: constant air density. Report CASA 05-16 of the Department of Mathematics and Computer Science, Eindhoven University of Technology (2005).

[5] D. Bežanović, E.F. Kaaschieter and C.J. van Duijn, Analysis of wet pressing of paper: the three-phase model. Part II: compressible air case. in preparation.

[6] J.F. Bloch and J.L. Auriault, Heat transfer in nonsaturated porous media: modelling by homogenisation, *Transport in Porous Media*, **30**: 301 – 321, 1998.

[7] F. El-Hosseiny, *Nordic Pulp and Paper Research Journal* 1 28, 1990.

[8] R. Helmig, *Multiphase Flow and Transport Processes in the Subsurface*, Springer, Berlin (1997).

[9] M. Kataja, K. Hiltunen, J. Timonen, Flow of water and air in a compressible porous medium. A model of wet pressing of paper, *J.Phys.D: Appl. Phys.* **25** (1992) 1053 – 1063.

[10] M. van Lieshout, Impulse drying in The Netherlands, TNO-report BU2.98/010158-2/ML, 1998.

[11] H. Paulapuro, Wet pressing-present understanding and future challenges, 12th Fundamental Research Symposium, Oxford (2001).

[12] J. Petrini, *On the Role of Evaporation Processes During Impulse Pressing of Paper*, Master's thesis, Lulea University of Technology, 2003.

[13] M. Riepen, An inside view on impulse drying phenomena by modelling, TAPPI Engineering conference, vol. 1, pp. 69-84, Anaheim, Canada, 1999.

[14] K.M. Singh, *Mathematical Analysis of the Wet Pressing of Paper*, PhD thesis, SUNY College of Environmental Science and Forestry, Syracuse, New York (1994).

[15] K. Velten and W. Best, Rolling of unsaturated porous materials: Evolution of fully saturated zone, *Physical Review E*, Volume **62**(3), 3891–3899, 2002.